Self Localization of Acoustic Sensor Networks

Randolph L. Moses, Robert M. Patterson, and Wendy Garber

Department of Electrical Engineering, The Ohio State University
2015 Neil Avenue, Columbus, OH 43210 USA

Abstract

We present algorithms for self-localization of a network of sensors. We consider the case when no "anchor" nodes with known locations are present. We use source signals in the scene, also at unknown locations, to estimate time-of-arrival and direction-of-arrival between sources and sensors. These measurements are used to compute maximum likelihood relative calibration solutions, in which sensor nodes are localized and oriented with respect to one another. Prior location information, in the form of uncertain aimpoints for a subset of the sensors, are then be used to obtain maximum *a posteriori* estimates of absolute locations and orientations. We derive analytical statistical performance bounds for the two estimators, and present examples that illustrate the performance of the algorithms.

1. Introduction

Sensor networks are becoming increasingly important for distributed sensing in a large number of military and nonmilitary applications [1]. A sensor network consists of a large number of low-cost, self-powered sensors that are capable of sensing signals, processing those signals, and communicating with other sensors or higher-level processing centers for data fusion and collaborative decision making.

In order to effectively fuse sensor information, it is often important to know the location and orientation of each sensor in the network. However, accurate sensor location and orientation is difficult to provide in many types of sensor deployment. Thus, there is interest in developing methods to find the locations and orientations (that is, to self-calibrate the sensor network) after the sensors have been deployed.

Self-localization in sensor networks is an active area of current research (see, *e.g.*, [2, 3, 4, 5] and the references therein). Iterative multilateration-based techniques are considered in [5]. Bulusu *et al.* [2, 6] consider a low-cost localization methods that use a number of beacon signals at known locations. Research on blind beamforming considers a related problem of forming a maximum power beam to a source without computing the source locations [7]. Cevher and McClellan consider sensor network self-calibration using

a single acoustic source that travels along a straight line [8]. Bearings-only localization methods for sensor networks are considered in [9].

In many self-calibration approaches it is assumed that there are one or more “beacons”, which are signal sources at known locations. The beacon signals are used to estimate the locations of some sensors; these sensors can then become beacons for locating other sensors. In other cases, some of the sensors are assumed to have known locations, and again other sensors are calibrated from these initially-known nodes. However, in many applications, the assumption of even a few nodes or beacons with known locations is difficult to satisfy. In military applications where sensors (and source signals) are deployed remotely, accurate location of even a small number of sensors or sources is difficult or impossible to achieve.

This paper presents algorithms for self-calibration of sensors when no anchor nodes with known prior location are available. We develop statistically optimal estimates for relative calibration of sensors, where relative calibration refers to location and orientation of sensors with respect to one another. The self-localization approach employs a set of "calibration" sources that have been placed in the scene, also at unknown locations. These calibration sources may be signals of opportunity, or they may be signal sources designed for network calibration. Each source emits a signature at an unknown time. The source is detected by each array, and the time-of-arrival (TOA) and possibly also the direction-of-arrival (DOA) of that source is recorded. These recorded measurements form the data from which the calibration solution is obtained.

In addition, we consider the case where uncertain prior knowledge of sensor or source locations are available. Such prior information could be generated from an uncertain aimpoint used by the device that places the sensor. We develop algorithms that use this prior aimpoint knowledge, coupled with the calibration measurements, to obtain estimates of both the relative node locations and orientations, and the absolute locations and orientations. The sensor locations and orientation estimates are found as the Maximum A Posteriori (MAP) estimates from the available measurement data and prior aimpoint information.

We partition the solution into relative calibration and absolute calibration. Relative calibration is important for such applications as locating and tracking targets. The relative accuracy of the sensor locations determine the target location and track errors relative to the sensor network. If the calibration signals are correctly designed, high relative accuracy can be achieved. Absolute calibration places the entire network scene on an absolute frame of reference. The absolute location accuracy is to a large part determined by the accuracy of the prior aimpoint information, and may be (much) less accurate than the relative calibration. On the other hand, posterior knowledge (such as the association of a relative target track to a road) can be used to refine the absolute calibration in a computationally efficient way.

We derive statistical uncertainty bounds on the localization estimates. The uncertainty analysis allows one to analytically predict the calibration performance in a number of scenarios of interest. Uncertainty bounds for both the relative and absolute calibration solutions are obtained.

Finally, we illustrate the proposed techniques with numerical examples, and explore the effect of sensor density and prior knowledge on calibration accuracy.

2. The Self-Calibration Problem

We consider a sensor deployment architecture as shown in Figure 1. A number of low-cost sensors, each equipped with a local processor, a low-power wireless communication transceiver, and one or more sensing capabilities, is set out in a region. Sensor elements may collect acoustic, seismic, and/or image data. Each sensor monitors its environment to detect, track, and characterize signatures. The sensed data is processed locally, and the result is transmitted to a local Central Information Processor (CIP) through a wireless communication network. The CIP fuses sensor information and transmits the processed information to a more distant command center. The wireless communication network is capable of proving a reference time base at each sensor. The CIP is also capable of computing a self-calibration solution from sensor measurements.

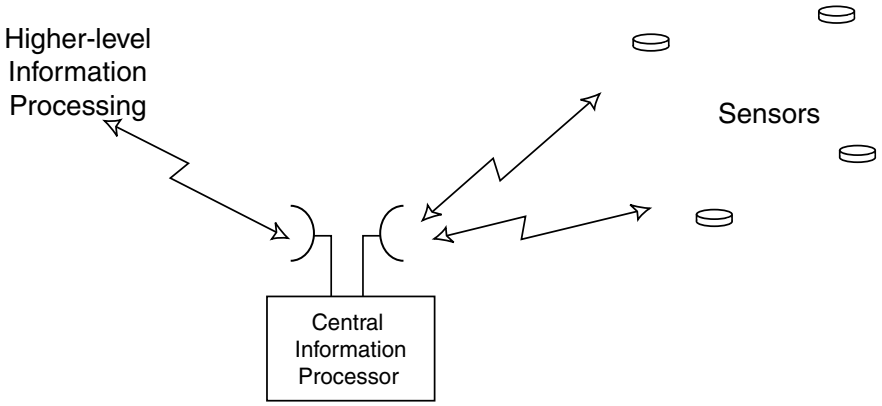

Figure 1: Sensor network architecture. A number of low-cost sensors are deployed in a region. Each sensor communicates to a local CIP, which relays information to a higher-level information processing center.

Assume we have a set of A sensors in a plane, each with unknown location $\{r_i = (x_i, y_i)\}_{i=1}^{A}$ and unknown orientation angle θ_i with respect to a reference direction (*e.g.*, North). In the array field are also placed S point source signals at unknown locations $\{\tilde{r}_j = (\tilde{x}_j, \tilde{y}_j)\}_{j=1}^{S}$. The sources may be co-located with sensors; such would be the case if sensors are equipped with a signal generator. Each source emits a signal that begins at time t_j. The signal emission times are generally assumed to be unknown. However, the t_j values could be known in some applications, such as if the sources can be electronically triggered or if they are co-located with sensors.

We each emitted source signal is detected by a subset of the sensors in the field. We assume that sensor i, if it detects source j, obtains an estimate of the time-of-arrival (TOA) t_{ij}. The TOA is measured with respect to a time base established across the sensor network using the RF communication link [] or by synchronizing the sensor processor clocks before deployment. We assume that errors in the time base are small compared to errors in the TOA estimates. The TOA estimate is obtained by using, for example, a generalized cross-correlator [10].

We assume that some sensor nodes can also estimate the direction-of-arrival (DOA) of an incoming source signal. In this case, if sensor i detects source j, we assume it estimates and direction-of-arrival (DOA) θ_{ij} of the source with respect to a local reference frame. The local reference frame could be, for example, "counter-clockwise from microphone #1" for an acoustic sensor with several microphones. DOA estimates cannot be made with respect to an absolute frame of reference because the orientation angle of each sensor node is unknown (and must be estimated in the calibration procedure).

The set of TOA and DOA measurements are gathered in a measurement vector

$$X = \left[\begin{array}{c} \mathrm{vec}(T) \\ \mathrm{vec}(\Theta) \end{array} \right]^T \quad (nx \times 1) \tag{1}$$

where $\mathrm{vec}(M)$ stacks the elements of a matrix M columnwise and where T and Θ contain the t_{ij} and θ_{ij} estimates for those source-sensor pairs for which a signal is detected. If all sensors detect all sources, then

$$T = \left[\begin{array}{cccc} t_{11} & t_{12} & \dots & t_{1S} \\ t_{21} & t_{22} & \dots & t_{2S} \\ \vdots & \vdots & \ddots & \vdots \\ t_{A1} & t_{A2} & \dots & t_{AS} \end{array} \right], \qquad \Theta = \left[\begin{array}{cccc} \theta_{11} & \theta_{12} & \dots & \theta_{1S} \\ \theta_{21} & \theta_{22} & \dots & \theta_{2S} \\ \vdots & \vdots & \ddots & \vdots \\ \theta_{A1} & \theta_{A2} & \dots & \theta_{AS} \end{array} \right] \tag{2}$$

and $nx = 2AS$. In many cases, though, not all sensor nodes detect all source signals, so some elements of T and Θ will be missing.

Each array transmits its TOA and DOA measurements to a central information processor, and these nx measurements form the data with which the CIP computes the sensor and source locations, the sensor orientations, and the source signal emission times. Note that the communication cost to the CIP is low, and the calibration processing is entirely performed by the CIP. Alternately, decentralized calibration solutions can be used [11] at the expense of higher intra-node communication costs.

Define the parameter vector

$$\alpha = [x_1,\, y_1,\, \theta_1, \dots, x_A,\, y_A,\, \theta_A | \tilde{x}_1,\, \tilde{y}_1,\, t_1, \dots, \tilde{x}_S,\, \tilde{y}_S,\, t_S]^T \quad (n\alpha \times 1) \tag{3}$$

where $n\alpha = 3(A + S)$. If any parameters in α are known, they are removed from α and the vector size reduces accordingly. For example, if we assume the sources and sensors are co-located, then $x_i = \tilde{x}_i$ and $y_i = \tilde{y}_i$, so α reduces to a $4A \times 1$ vector ($3A \times 1$ if the t_j's are assumed to be known).

The actual TOA and DOA of source signal j at sensor i can be computed from α as

$$\tau_{ij}(\alpha) = t_j + \|r_i - \tilde{r}_j\|/c \tag{4}$$

$$\phi_{ij}(\alpha) = \theta_i + \angle(r_i, \tilde{r}_j) \tag{5}$$

respectively, where $\|\cdot\|$ is the Euclidean norm, $\angle(\xi, \eta)$ is the angle between the points $\xi, \eta \in \mathcal{R}^2$, and c is the signal propagation velocity. We assume that the propagation velocity c is known; methods for estimating c can be found in [7, 12].

Measurement Uncertainty: Each element of X has measurement uncertainty; we model the uncertainty as

$$X = \mu(\alpha) + E \tag{6}$$

where $\mu(\alpha)$ is the noiseless measurement vector whose elements are given by equations (4) and (5) for values of i, j that correspond to the vector stacking operation in (1), and where E is a random vector, giving a measurement vector probability density function (pdf) denoted as $f_X(x; \alpha)$.

We will adopt a Gaussian measurement error model; that is, we will assume that

$$f_X(x; \alpha) = \mathcal{N}(\mu(\alpha), \Sigma_X) \tag{7}$$

where Σ_X is a known covariance matrix. We justify this assumption by noting that for sufficiently high signal-to-noise ratio, the TOA estimate is approximately Gaussian with standard deviation on the order of the inverse of the signal bandwidth [13]. In addition, for these signal-to-noise ratios, most DOA estimators are Gaussian. It is reasonable to assume that the TOA and DOA estimates computed at different sensors are uncorrelated with each other, so we will often assume that Σ_X is diagonal. We note that neither the Gaussian assumption nor the diagonal covariance assumption is needed in the derivations that follow; however, they make the exposition more concrete and they are the models employed in the simulations presented in Section 6.

Prior Information: In addition to the calibration measurements, one often has some prior information about sensor or source locations. For example, if a subset of sources or sensors is equipped with GPS prior location information for these sources or sensors is available. If sensors or sources are placed by air drop or by artillery fire, an aimpoint location for these sensors, along with some aimpoint uncertainty, may be available.

In most cases, the prior information contains uncertainty. For example, aimpoints of sensors have an associated uncertainty corresponding to the precision limit of the air drop or munition placement. GPS systems also provide uncertain location information; for GPS units not operating in differential mode, this uncertainty can be several meters. We quantify this uncertain prior information using a probability density function $f_0(\alpha)$. As an example, one can assume $f_0(\alpha)$ is Gaussian distributed with known mean and covariance, so

$$f_0(\alpha) = \mathcal{N}(\alpha_0, \Sigma_0) \tag{8}$$

where α_0 and Σ_0 are given. In this case, α_0 encodes the aimpoints and Σ_0 encodes the aimpoint uncertainty.

The self-calibration problem, then, is: Given the measurement vector X, measurement error pdf $f_X(x;\alpha)$, and prior information pdf $f_0(\alpha)$, estimate α.

3. Absolute and Relative Calibration

We will partition the calibration solution into a *relative calibration* and an *absolute calibration*. Relative calibration is location and orientation calibration of sensors (and sources) relative to one another, while absolute calibration is the calibration with respect to an absolute frame of reference. This partitioning of the problem is useful for several reasons:

1. In many cases the error covariance of α has high marginal variances and high correlation between its entries, due largely to errors associated with translation and rotation of the entire network. By partitioning this error into a relative and overall translation-rotation error, we find that the relative error is smaller, has lower correlation among its entries, and is only weakly coupled to the translation and rotation errors. The partitioning thus provides a convenient and intuitive decomposition of the error into its primary components.

2. The TOA and DOA measurement used for calibration of the sensor network provide information about relative calibration only.

3. For many military sensing applications, such as target localization and tracking, the performance depends on how accurately the sensors are located with respect to each other; thus, relative calibration is of interest when assessing target location or tracking errors due to sensor location uncertainties.

4. Absolute calibration can be updated using additional information which may not be available during the initial sensor network calibration stage. As an example, associating a target track to a road may result in absolute calibration refinement, leaving the relative calibration unaltered.

We decompose the calibration parameter vector α into its relative and absolute components as follows. Define the centroid location and orientation of the sensor nodes as, $\alpha_c(\alpha) = [x_c, y_c, \theta_c]^T$, where

$$x_c = \frac{1}{A}\sum_{i=1}^{A} x_i \qquad y_c = \frac{1}{A}\sum_{i=1}^{A} y_i \qquad \theta_c = \frac{1}{A}\sum_{i=1}^{A} \theta_i \tag{9}$$

The mapping from a parameter vector α to α_c can be written in matrix form as

$$\alpha_c = B\alpha \tag{10}$$

where B is the $(3 \times n_\alpha)$ matrix defined as

$$B = \frac{1}{A}[\underbrace{I_3\ I_3\ \cdots\ I_3}_{A} \mid \underbrace{0\ 0\ \cdots\ 0}_{S}] \tag{11}$$

and where I_3 is the (3×3) identity matrix and 0 is the (3×3) matrix of zeroes. Given α_c, the mapping from α to α_r is a translation and rotation such that

$$B\alpha_r = 0 \tag{12}$$

The transformation is defined as follows for a vector α with centroid $\alpha_c = [x_c, y_c, \theta_c]^T$. For the ith sensor with parameters (x_i, y_i, θ_i), which are the $3(i-1)+1$ to $3(i-1)+3$ elements of α, the corresponding elements of α_r are given by

$$\begin{bmatrix} x_{i,r} \\ y_{i,r} \\ \theta_{i,r} \end{bmatrix} = \begin{bmatrix} \cos\theta_c & \sin\theta_c & 0 \\ -\sin\theta_c & \cos\theta_c & 0 \\ 0 & 0 & 1 \end{bmatrix} \begin{bmatrix} x_i - x_c \\ y_i - y_c \\ \theta_i - \theta_c \end{bmatrix} \tag{13}$$

Similarly, the elements of α_r corresponding to the jth source are given by

$$\begin{bmatrix} \tilde{x}_{j,r} \\ \tilde{y}_{j,r} \\ t_{j,r} \end{bmatrix} = \begin{bmatrix} \cos\theta_c & \sin\theta_c & 0 \\ -\sin\theta_c & \cos\theta_c & 0 \\ 0 & 0 & 1 \end{bmatrix} \begin{bmatrix} \tilde{x}_j - x_c \\ \tilde{y}_j - y_c \\ t_j \end{bmatrix} \tag{14}$$

Thus, there is a one-to-one relationship between a parameter vector α and the two vectors α_r and α_c. Note that t_j remains unchanged by the transformation. The inverse transformations are readily obtained from (13)–(14). We will use α and (α_r, α_c) interchangeably in the remainder of the paper.

4. MAXIMUM A POSTERIORI CALIBRATION ALGORITHMS

In this section we present algorithms for computing the relative and absolute calibration from TOA and DOA estimates along with prior aimpoint information. Relative calibration refers to estimating α_r, and absolute calibration refers to estimating α, or equivalently, to estimating (α_r, α_c).

We consider α as a random vector with prior probability density function $f_0(\alpha)$. The measurement vector X informs us about α as quantified by the posterior probability $f(\alpha|X)$. From Bayes' rule,

$$f(\alpha|X) = \frac{f(X|\alpha)f_0(\alpha)}{f(X)} \tag{15}$$

We choose as our estimate maximum *a posteriori* (MAP) estimate, which is the value of α that maximizes the posterior probability density of α:

$$\hat{\alpha} = \arg\max_{\alpha} f(\alpha|X) = \arg\max_{\alpha} f(X|\alpha)f_0(\alpha) \tag{16}$$

The calibration measurements X are independent of absolute location. Any translation or rotation of the entire sensor-source scene results in no change to the distances from sources to sensor nor the relative angles of sources from sensors. Thus, $f(X|\alpha) = f(X|\alpha_r)$. Combining this fact with the negative logarithm of equation (16) yields

$$\hat{\alpha} = \arg\min_{(\alpha_r,\alpha_c)} [-\ln f(X|\alpha_r) - \ln f_0(\alpha)] \tag{17}$$

Equation (17) is valid for any measurement and prior pdfs. For the case of Gaussian pdfs in equations (7)–(8), equation (17) becomes

$$\hat{\alpha} = \arg\min_{(\alpha_r,\alpha_c)} [X - \mu(\alpha)]^T \Sigma_X^{-1} [X - \mu(\alpha)] + [\alpha - \alpha_0]^T \Sigma_0^{-1} [\alpha - \alpha_0] \tag{18}$$

If in addition the measurement errors are uncorrelated, and if the the TOA and DOA measurement errors have variances σ_t^2 and σ_θ^2, respectively, then

$$[X - \mu(\alpha)]^T \Sigma_X^{-1} [X - \mu(\alpha)] = \frac{1}{\sigma_t^2} \sum_{(i,j)\in D_T} (t_{ij} - \tau_{ij}(\alpha))^2 + \frac{1}{\sigma_\theta^2} \sum_{(i,j)\in D_\Theta} (\theta_{ij} - \phi_{ij}(\alpha))^2 \tag{19}$$

where D_T is the set of (i, j) pairs for which sensor i estimates the TOA of source j, and D_Θ is the set of (i, j) pairs for which sensor i estimates the DOA of source j.

Equation (18) gives the MAP estimate of α when both measurements and prior information are available.

We next consider the case in which no prior information is available. In this case we seek a maximum likelihood (ML) estimate; that is, we find $\alpha \leftrightarrow (\alpha_r, \alpha_c)$ that maximizes $f(X|\alpha) = f(X|\alpha_r, \alpha_c)$. Note, however, that this pdf is independent of α_c, so

$$f(X|\alpha_r, \alpha_c) = f(X|\alpha_r) \tag{20}$$

Thus, there are an infinite number of ML estimates, all with the same α_r vector and differing only by their centroid α_c. We can thus find a unique *relative* calibration as the maximum likelihood solution

$$\hat{\alpha}_{r,ML} = \arg\max_{\alpha_r} f(X|\alpha_r) = \arg\min_{\alpha_r} [-\ln f(X|\alpha_r)] \tag{21}$$

where α_r is constrained to satisfy equation (12).

Both equation (18) and equation (21) involve minimization of a nonlinear function of α; for the Gaussian case, these equations yield nonlinear least squares minimization problems. In the next section we discuss various approaches to solve these minimization problem.

4.1 ALGORITHMS FOR SELF-CALIBRATION

4.1.1 Relative Calibration

Let us first consider the solution of equation (21). We can write this as

$$\hat{\alpha}_{r,ML} = \arg\min_{\alpha_r} J_1(\alpha_r) \text{ subject to } B\alpha_r = 0 \tag{22}$$

where

$$J_1(\alpha_r) = -\ln f(X|\alpha_r) \tag{23}$$

In the Gaussian measurement error case, $J_1(\alpha_r) = \frac{1}{2}[X - \mu(\alpha)]^T \Sigma_X^{-1} [X - \mu(\alpha)]$. The minimization can be found by iterative descent of α_r from an initial estimate; however, since there is no prior information about α_r, one must be careful to find an initial estimate that is in the attraction region of the global minimum of $J_1(\alpha_r)$.

Our solution is based on an ML estimator described in [14, 15]. Note that there is a one-to-one correspondence between a parameter vector α_r and a parameter vector α_1 for which $x_1 = y_1 = \theta_1 = 0$, and one can compute α_r from α_1 using a rotation and translation such that $B\alpha_r = 0$; the transformation equations are similar to (13)–(14). We use the fact that if $\hat{\alpha}$ is an ML estimate of α and $g(\cdot)$ is a one-to-one mapping, then $g(\hat{\alpha})$ is an ML estimate of $g(\alpha)$ [16]. Thus, an ML estimate of α_r can be found by computing an ML estimate of α_1 and transforming it to its corresponding α_r vector. An algorithm for finding the ML estimate of α_1 is described [15]. The algorithm includes an computationally efficient initialization followed by a nonlinear descent.

It is interesting to note that the ML estimate of the relative calibration can be found by assuming one sensor node has known location and orientation and then finding the ML estimate of the remaining sensors.

4.1.2 Absolute Calibration

We next consider algorithms for finding the MAP absolute calibration estimate. We can write equation (17) as

$$\hat{\alpha} = \arg\min_{(\alpha_r, \alpha_c)} [J_1(\alpha_r) + J_2(\alpha_r, \alpha_c)] \tag{24}$$

where $J_1(\alpha_r) = -\ln f(X|\alpha_r)$ and $J_2(\alpha_r, \alpha_c) = -\ln f_0(\alpha)$. In the Gaussian case J_1 and J_2 are given by the quadratic forms on the right side of equation (18), to within an additive constant.

Consider first the case for which the prior information on α is known with relatively high accuracy. In this case one can exploit the prior information to determine an initial estimate α, which form a starting point for the nonlinear minimization. For example, if we know the prior locations of at least two sensors with high accuracy, then the techniques developed in [15] can be used to initialize the locations orientations, and emission times of the sources and sensors. In essence, those nodes known with high accuracy form beacon nodes from which other initial node locations and orientations can be estimated.

Next, consider the case in which which the prior location information has (very) high uncertainty. In this case, J_2 varies slowly as a function of α_r in comparison with $J_1(\alpha_r)$. We can thus obtain an initial estimate by minimizing J_1 only. But this minimization is exactly the ML relative calibration solution given in equation (22). Once $\hat{\alpha}_r$ is obtained, we need only to initialize the 3×1 centroid vector α_c. One way to do so is to to find the translation components x_c and y_c to align the centroid of the sensor and source locations to centroid of the prior location information, then to search over θ_c on the interval $[0, 2\pi)$ to minimize $J_2(\hat{\alpha}_r, \alpha_c)$. Another approach that avoids the one-dimensional search is to find the rotation, translation, and scaling of the nodes in α_r that aligns them to aimpoint centroids of the corresponding nodes for which prior location information is available. The solution can be solved for in closed-form using a least-squares estimate [17]. The rotation and translation estimates can be used as an initial estimate of α_c.

In all cases above, once initial estimates of α_r and α_c are found, one can find $\hat{\alpha}$ from (24) using an iterative descent procedure. In our implementation we used the Matlab function `lsqnonlin`.

If the prior knowledge has high uncertainty, an approximate MAP solution may be found by solving separately for $\hat{\alpha}_r$ and $\hat{\alpha}_c$ in equation (24) as:

$$\hat{\alpha}_r \approx \arg\min_{\alpha_r} J_1(\alpha_r) \tag{25}$$

$$\hat{\alpha}_c \approx \arg\min_{\alpha_c} J_2(\hat{\alpha}_r, \alpha_c) \tag{26}$$

Note that (25) is exactly the ML relative calibration solution, and (26) is a solution over only three parameters.

The decoupling of the α_r and α_c estimates as in equations (25)–(26) has another advantage. If additional absolute location information becomes available after the calibration process, one can simply update $\alpha_c = [x_c, y_c, \theta_c]$ without changing the calibration estimate of α_r. An example of such additional information could be an association of a target track with a nearby road. By placing the target on the road, one develops a correction for the overall sensor network translation and orientation (that is, a correction for α_c) that does not affect α_r. For such sensor network as target location and tracking, there is a natural and functional argument for partitioning of the self-calibration problem into the internal (to the network) problem of relative calibration and the external problem of absolute location of the entire sensor network, treated as a rigid body.

5. ESTIMATION ACCURACY

In this section we derive analytical lower bounds on the estimation variance for both the maximum likelihood estimate of the relative calibration vector α_r and for the MAP estimate of α that incorporates both the calibration measurements and the prior location information. The bounds are tight in the sense that the ML and MAP estimates achieve those bounds for high measurement signal-to-noise ratio.

5.1 Estimation Accuracy of Relative Location

We first derive a lower bound on the covariance of any unbiased estimator of α_r based on measurements X. In this derivation, we assume no prior knowledge on α, which is equivalent to assuming that α is a deterministic unknown parameter vector [16]. Since X provides no information about the centroid parameter vector α_c, we find that the Fisher information matrix of α is singular and no (finite) variance lower bound exists. However, we can compute a lower bound on the variance of α_r, using the constrained estimator bounds presented in [18, 19, 20, 21]. It turns out that the tangent space of the constraints imposed on α_r correspond exactly to the the null space of its Fisher information matrix, so a finite variance bound is obtained except in degenerate cases. Degenerate cases occur with probability zero; an example is when all sensors are collinear and a calibration source is collinear with the sensors and not between any two sensors; in this case, the location variance bound of the sensors is finite, but the location bound of the collinear source is infinite in the collinear direction.

The Fisher Information Matrix of α is given by [16]

$$I_\alpha = E\left\{ \left[\nabla_\alpha \ln f_X(X;\alpha)\right] \left[\nabla_\alpha \ln f_X(X;\alpha)\right]^T \right\}$$

For the Gaussian estimation error case, the partial derivatives are readily computed from equation (7) to give

$$I_\alpha = [G'(\alpha)]^T \Sigma_X^{-1} [G'(\alpha)] \tag{27}$$

where $G'(\alpha_1)$ is the $nx \times n\alpha$ matrix whose ijth element is $\partial\mu_i(\alpha_1)/\partial(\alpha_1)_j$, computed from equations (4) and (5).

The Fisher Information Matrix is rank deficient due to the translational and rotational ambiguity in the self-calibration solution [15]. However, the CRB of α_r is finite, and given by [20]:

$$E\{[\hat{\alpha}_r - \alpha_r][\hat{\alpha}_r - \alpha_r]^T\} \geq C_{\alpha_r} = U\left(U^T I_\alpha U\right)^{-1} U^T \tag{28}$$

where U is an $n\alpha \times (n\alpha - 3)$ matrix satisfying

$$U^T U = I \tag{29}$$

$$UU^T = P_M^\perp = I - M\left(M^T M\right)^{-1} M^T \tag{30}$$

and where M is the $n\alpha \times 3$ matrix defined by

$$M = \left[\begin{array}{ccc|ccc} M_1 & M_2 & \cdots & M_A & \tilde{M}_1 & \tilde{M}_2 & \cdots & \tilde{M}_S \end{array}\right]^T \tag{31}$$

$$M_i = \begin{bmatrix} 1 & 0 & 0 \\ 0 & 1 & 0 \\ -y_i & x_i & 1 \end{bmatrix}, \qquad \tilde{M}_j = \begin{bmatrix} 1 & 0 & 0 \\ 0 & 1 & 0 \\ -\tilde{y}_j & \tilde{x}_j & 0 \end{bmatrix} \tag{32}$$

If $\left(U^T I_\alpha U\right)$ is singular in equation (28), more general bounds can be used [21].

When the CRB of α_r is finite, it can be instead computed using an eigendecomposition of I_α. Let

$$I_\alpha = [U_1 U_2] \begin{bmatrix} \Lambda & 0 \\ 0 & 0 \end{bmatrix} \begin{bmatrix} U_1^T \\ U_2^T \end{bmatrix} \tag{33}$$

where U_2 is an $(n \times 3)$ matrix. Then the CRB of α_r is given by the pseudoinverse of I_α:

$$C_{\alpha_r} = U_1 \Lambda^{-1} U_1^T \tag{34}$$

5.2 Covariance Bound for Absolute Location Estimation

For the case of Gaussian prior information, covariance of the MAP estimate $\hat{\alpha}$ from (24) is given by [16]

$$E\left\{[\hat{\alpha} - \alpha][\hat{\alpha} - \alpha]^T\right\} \geq [\Sigma_0^{-1} + I_\alpha]^{-1} \tag{35}$$

where I_α is given by equation (27). For nonGaussian priors, a similar equation involving partial derivatives of $\ln f_0(\alpha)$ can be obtained.

An interpretation of the above result is as follows. Since the prior information and the measurement information are independent, the information matrix for α is the sum of the individual information matrices. The Fisher information matrix for the Gaussian prior with covariance Σ_0 is Σ_0^{-1}. The Fisher information from the measurements is I_α, and equation (35) follows.

We note that equation (35) involves an expectation over both the random variable α and the random measurement errors. If one is interested in the calibration error for a fixed realization of α, one can compute a variance bound on α_r to bound relative calibration for this realization, then include the (now fixed) centroid errors for this realization.

6. Numerical Results

This section presents numerical examples of the self-calibration procedure. First, we present a synthetically-generated example consisting of ten sensors and eleven sources placed randomly in a 2 km$\times$2 km region. Second, we present results from field measurements using acoustic sources and sensors.

6.1 Synthetic Data Example

We consider a case in which ten sensors are randomly placed in a 2 km$\times$2 km region. In addition, eleven sources are randomly placed in the same region. In both cases the nominal locations of the sensors and sources are first randomly chosen. Then, the actual locations are chosen as random Gaussian perturbations from the nominal locations, where the perturbation is found by adding Gaussian noise with zero mean and standard deviation of 10 meters to each location. The sensor orientations and source emission times are also randomly chosen. Figure 2 shows the actual locations of the sensors and sources.

Next, TOA and DOA measurements are simulated. We assume every sensor detects each source emission and measures the TOA and DOA of the source. The measurement uncertainties are Gaussian with standard deviations of $\sigma_t = 1$ msec for the TOAs and $\sigma_\theta = 3^\circ$ for the DOAs. Neither the locations nor emission times of the sources are assumed to be known.

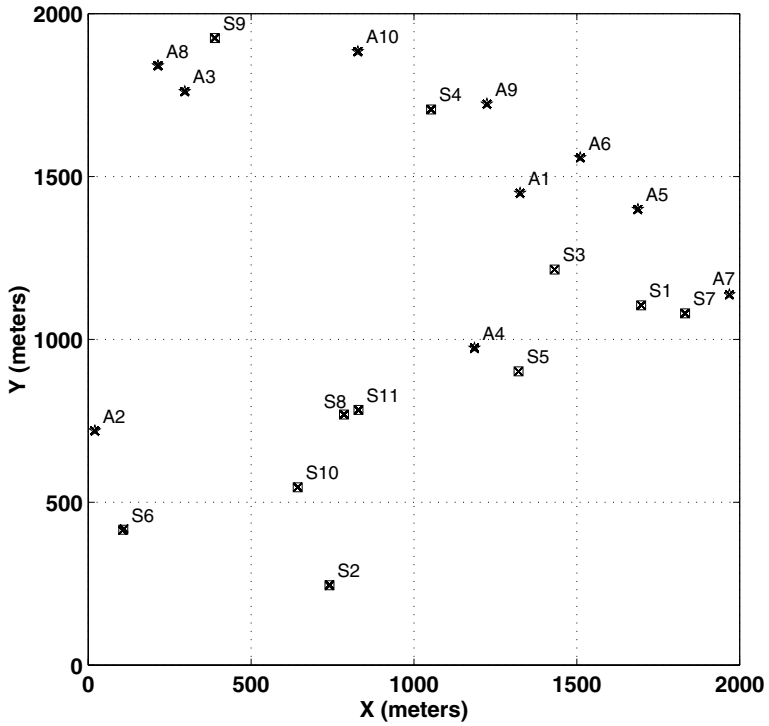

Figure 2: Top: Example scene showing ten sensors A1–A10 (stars) and eleven sources S1–S11 (squares). Also shown are the 2σ location uncertainty ellipses of the sensors and sources; these are on average less than 0.5 m in radius and show as small dots. Bottom: enlarged views near sensors A6 and A8, showing 2σ location uncertainty ellipses along with location estimates from 200 Monte-Carlo experiments.

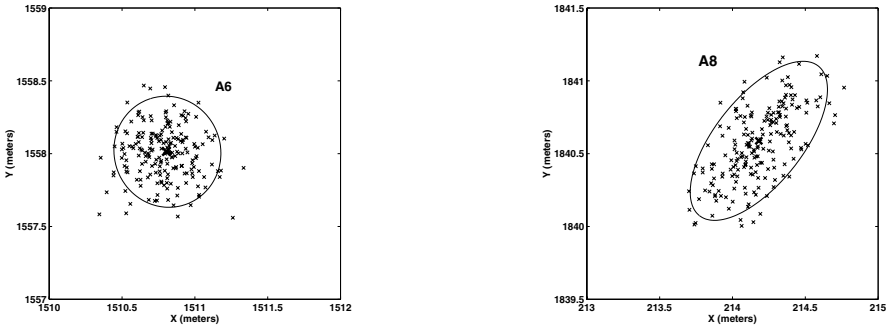

Figure 3: Two standard deviation location uncertainty ellipses for sensors $A6$ and $A8$ from Figure 2.

Figure 2 also shows the two standard deviation (2σ) location uncertainty ellipses for the relative location estimates of both the sources and sensors. The ellipses are obtained from the 2×2 covariance submatrices of the CRB in equation (34) that correspond to the relative location parameters in α_r of each sensor or source. These ellipses appear as small dots in the figure; enlarged views for two sensors are also shown.

The results of the maximum likelihood estimation of relative location are also shown in Figure 3. The 'x' marks show the ML location estimates from 200 Monte-Carlo experiments with randomly-generated DOA

Table 1: Average 2σ uncertainty radius for relative and absolute sensor calibration for the example presented

	Theoretical Value	Monte-Carlo Simulation
Relative Location	0.47 m	0.43 m
Absolute Location	5.09 m	5.19 m

and TOA measurements. The DOA and TOA measurement errors were drawn from Gaussian distributions with zero mean and variances of $\sigma_t = 1$ msec and $\sigma_\theta = 3^\circ$, respectively. The ellipse shows the 2-standard deviation (2σ) relative location uncertainty region as predicted from the CRB. We find good agreement between the CRB uncertainty predictions and the Monte-Carlo experiments, which demonstrates the statistical efficiency of the ML estimator for this level of measurement uncertainty.

We summarize the ten location uncertainty ellipses into a single quantity by first defining the sensor or source 2σ *uncertainty radius* as the radius of a circle whose area is the same as the area of the 2σ location uncertainty ellipse. The 2σ uncertainty radius for each sensor or source is computed as the geometric mean of the major and minor axis lengths of the 2σ uncertainty ellipse. We then find the RMS value of these uncertainty radii to obtain a single average location error measure. Table 1 shows the average 2σ uncertainty ellipse radius for the ten sensors, as computed from the CRB, and also the estimated average uncertainty ellipse computed from Monte-Carlo experiments. The Monte-Carlo results are found by estimating α_r for each of the 200 Monte-Carlo experiments. We also compute the true α_r vector by transforming the true α vector so that its centroid is zero. In each Monte-Carlo experiment we compute the average distance from each sensor to its corresponding true relative location, then average this distance over all Monte-Carlo experiments. We see that the results agree, and the average uncertainty radius is approximately 0.45 m for this example. Not shown in the figure are the sensor orientation angles and their estimates; the 2σ angle error bound, predicted from the CRB, is 1.8° for each sensor, and the Monte-Carlo estimates are close to this value as well.

We also estimate the absolute location and the average location error. In this case we compute $\hat{\alpha}$ for each of the 200 Monte-Carlo experiments and then compute the average distance from the true locations as above. We compare this average 2σ error distance to the corresponding average error computed from $\text{cov}(\hat{\alpha})$ in equation (35). These results are also shown in Table 1. We see that the absolute 2σ error is about 5 meters, approximately one-fourth the prior 2σ uncertainty of 20 meters for each sensor.

This experiment shows that relative location calibration of the sensors to errors well less than 1 meter is possible. In addition, even with weak prior information of sensor locations, as might be available from aimpoints for sensor placement, absolute location uncertainties on the order of 5 meters can be obtained. It is significant that the relative location errors are small — this means that beamforming or source location and tracking can be expected to have high accuracy. The absolute location corresponds to uncertainty only in the translation or rotation of the entire sensor network. While this leads to a corresponding uncertainty in, for example, a target being tracked by the network, the uncertainty lies largely in the translation and rotation of the track. Other available information may be used to further correct for this location and translation error. If a track is found to be slightly translated and rotated from a known road, for example, the absolute orientation sensor network can be correspondingly adjusted.

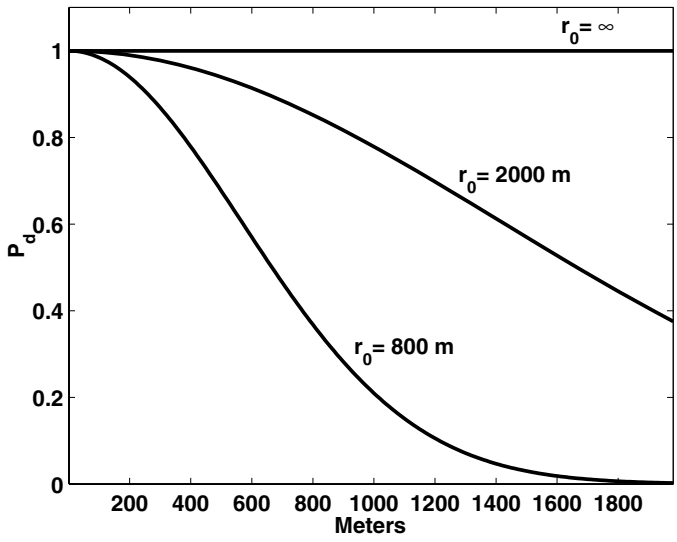

Figure 4: Detection probability of a source a distance r from a sensor, for three values of r_0.

Partial Measurements

Next, we consider the case when not all sensors detect all sources. For a sensor that is a distance r from a source, we model the detection probability as

$$P_D(r) = \exp^{-(r/r_0)^2} \tag{36}$$

where r_0 is a constant that adjusts the decay rate on the detection probability (r_0 is the range in meters at which $P_D = e^{-1}$). We assume that when a sensor detects a source, it measures both the DOA and TOA of that source.

Three detection probability profiles are considered, as shown in Figure 4, and correspond to $r_0 = 800\,\text{m}$, $r_0 = 2000\,\text{m}$, and $r_0 = \infty$. Figure 5 shows the average 2σ uncertainty radius values, computed from the inverse of the FIM, for each of these choices for r_0. In this experiment we assume the locations of sensors A1 and A2 are known. The average number of sources detected by each sensor is also shown. For $r_0 = 2000\,\text{m}$ we see only a slight uncertainty increase over the case where all sensors detect all sources. When $r_0 = 800\,\text{m}$ the average location uncertainty is substantially larger, because the effective number of sources seen by each sensor is small. This behavior is consistent with the average number of sources detected by each sensor, shown in the figure. For a denser set of sensors or sources, the uncertainty reduces to a value much closer to the case of full signal detection; for example, with 30 sensors and 30 sources in this region the average uncertainty is less than 1 m even when $r_0 = 800\,\text{m}$.

6.2 Field Test Results

We present the results of applying the auto-calibration procedure to an acoustic source calibration data collection conducted during the DUNES test at Spesutie Island, Aberdeen Proving Ground, Maryland in September 1999. In this test, four acoustic sensors are placed at known locations 60-100 m apart as shown in Figure 6. Four acoustic source signals are also used. Exact ground truth locations of the calibration sources

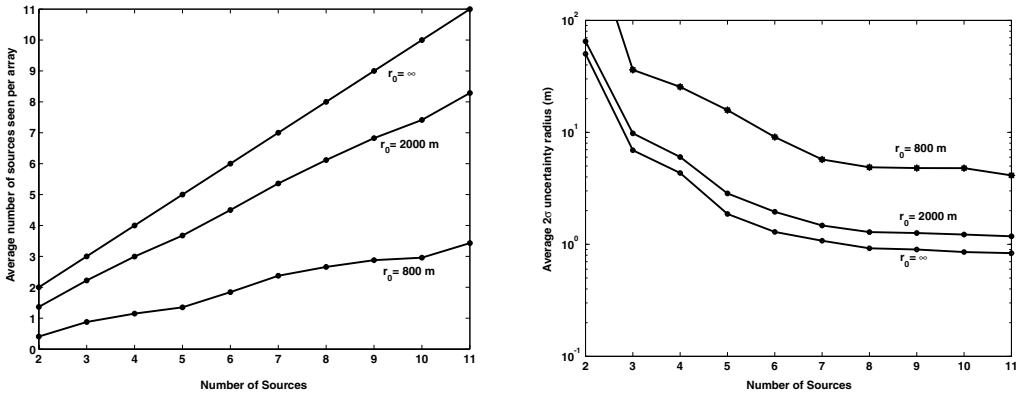

Figure 5: Left: Average 2σ location uncertainty for sensors in Figure 2 for three detection probability profiles. Right: Average number of sources detected by each sensor in each case.

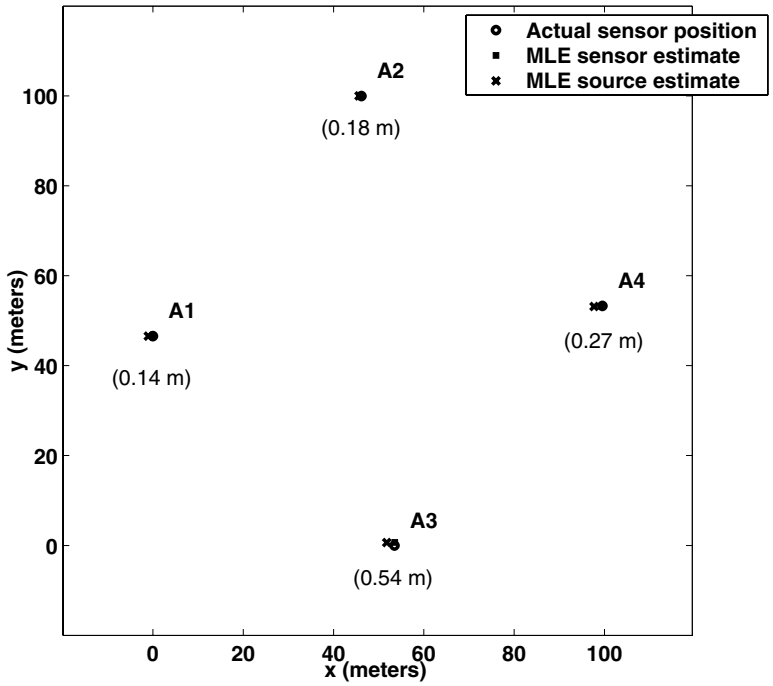

Figure 6: Actual and estimated sensor locations, and estimated source locations, using field test data. Error distances between actual and estimated sensor locations are shown in parentheses.

are not known, but it is known that each source is within approximately 1 m of a sensor. Each source signal is a series of bursts in the 40-160 Hz frequency band. Time-aligned samples of the sensor microphone signals are acquired at a sampling rate of 1005.53 Hz. Times of arrival are estimated by cross-correlating the measured microphone signals with the known source waveform, and finding the peak of the correlation function. Only a single microphone signal is available at each sensor, so while TOA measurements are obtained, no DOA measurements are available. Figure 6 shows the ML estimates of the relative sensor and source location, as compared to the known relative locations of the sensors. The location errors of sensors A1, A2, A3, and A4, are 0.14 m, 0.18 m, 0.54 m and 0.27 m, respectively, for an average error of 0.28 m. In addition, the source location estimates are within 1 m of the sensor locations, consistent with our ground truth information.

7. CONCLUSIONS

We have presented a procedure for calibrating the locations and orientations of a network of sensors when no sensors or calibration sources have known position. The calibration procedure uses source signals that are placed in the scene at unknown locations. The sensors detect the source signals and obtain a noisy measurement of the time-of-arrival and possibly also the direction-of-arrival of the source signal. These measurements, along with uncertain prior aimpoint information for sensors or sources, are estimates obtained for each source-sensor pair.

We consider both relative calibration and absolute calibration of the sensor networks. We partition the calibration problem into a relative calibration and an overall translation and rotation of the sensor network

scene. In relative calibration, sensor and source signal locations and sensor orientations are computed with respect to one another. Relative calibration requires no prior knowledge of sensor or source locations. The absolute calibration involves computing an overall scene translation and rotation from prior aimpoint information.

We present maximum likelihood solutions for the relative calibration, and show that it can be computed from an earlier maximum likelihood calibration that assumes one sensor has known location and orientation. We also present a maximum *a posteriori* estimate of the total calibration that combines calibration measurements with prior aimpoint knowledge. We show that if the prior knowledge has high uncertainty with respect to the measurement information, the total calibration partitions into separate relative calibration coupled with a single scene translation and rotation estimate. The latter estimate can be refined if post-calibration information, such as target track associations, are available.

We also derive statistical bounds on the calibration uncertatinty. We derive bounds for both relative calibration and absolute calibrations. The relative calibration bounds are useful because it is relative sensor location error that limits the location or track estimation accuracy in target tracking applications that employ the sensor network.

Numerical results show that the calibration estimators essentially achieve their respective lower bounds for the cases considered. Examples illustrating the effects of sensor density, partial detections of source signals, and co-location of sensors on calibration accuracy are presented. An initial result based on field measurements is encouraging.

Acknowledgement

This material is based in part upon work supported by the U.S. Army Research Office under Grant No. DAAH-96-C-0086 and Batelle Memorial Institute under Task Control No. 01092, and in part through collaborative participation in the Advanced Sensors Consortium sponsored by the U.S. Army Research Laboratory under the Federated Laboratory Program, Cooperative Agreement DAAL01-96-2-0001. Any opinions, findings, and conclusions or recommendations expressed in this publication are those of the authors and do not necessarily reflect the views of the U.S. Army Research Office, the Army Research Laboratory or the U.S. Government.

References

[1] "Collaborative signal and information processing in microsensor networks," *IEEE Signal Processing Magazine*, vol. 19, March 2002.

[2] N. Bulusu, J. Heidemann, and D. Estrin, "GPS-less low-cost outdoor localization for very small devices," *IEEE Personal Communication*, vol. 7, pp. 28–34, October 2000.

[3] C. Savarese, J. Rabaey, and J. Beutel, "Locationing in distributed ad-hoc wireless sensor networks," in *Proceedings of the International Conference on Acoustics, Speech, and Signal Processing*, vol. 4, (Salt Lake City, UT), pp. 2037–2040, May 2001.

[4] L. Griod and D. Estrin, "Robust range estimation using acoustic and multimodal sensing," in *IEEE/RSJ International Conference on Intelligent Robots and Systems*, (Maui, Hawaii), pp. 1312–1320, October 2001.

[5] A. Savvides, C. C. Han, and M. B. Srivastava, "Dynamic fine-grained localization in ad-hoc wireless sensor networks," in *Proceedings of the International Conference on Mobile Computing and Networking (MobiCom) 2001*, (Rome, Italy), July 2001.

[6] N. Bulusu, D. Estrin, L. Girod, and J. Heidemann, "Scalable coordination for wireless sensor networks: Self-configuring localization systems," in *Proceedings of the Sixth International Symposium on Communication Theory and Applications (ISCTA '01)*, July 2001.

[7] K. Yao, R. E. Hudson, C. W. Reed, D. Chen, and F. Lorenzelli, "Blind beamforming on a randomly distributed sensor array system," *IEEE Journal on Selected Areas in Communications*, vol. 16, pp. 1555–1567, October 1998.

[8] V. Cevher and J. H. McClellan, "Sensor array calibration via tracking with the extended kalman filter," in *Proceedings of the Fifth Annual Federated Laboratory Symposium on Advanced Sensors*, (College Park, MD), pp. 51–56, March 20–22 2001.

[9] L. Kaplan, L. Q. Le, and P. Molnar, "Maximum likelihood methods for bearings-only target localization," in *Proceedings of the International Conference on Acoustics, Speech, and Signal Processing*, vol. 5, (Salt Lake City, UT), pp. 3001–3004, May 2001.

[10] C. Knapp and G. C. Carter, "The generalized correlation method for estimation of time delay," *IEEE Transactions on Acoustics, Speech, and Signal Processing*, vol. 4, pp. 320–326, August 1976.

[11] A. Savvides, H. Park, and M. Srivastava, "The bits and flops of the n-hop multilateration primitive for node localization problems," in *First ACM International Workshop on Wireless Sensor Networks and Applications (WSNA 02)*, (Atlanta, GA), September 2002.

[12] R. L. Moses and R. M. Patterson, "Self-calibration of sensor networks," in *Unattended Ground Sensor Technologies and Applications IV (Proc. SPIE Vol. 4743)* (E. M. Carapezza, ed.), pp. 108–119, April1–4 2002.

[13] D. Krishnamurthy, "Self-calibration techniques for acoustic sensor arrays," Master's thesis, The Ohio State University, January 2002.

[14] R. L. Moses, D. Krishnamurthy, and R. M. Patterson, "An auto-calibration method for unattended ground sensors," in *Proceedings of the 2001 Battlefield Acoustics Symposium*, (Laurel, MD), October 23–25 2001.

[15] R. L. Moses, D. Krishnamurthy, and R. Patterson, "A self-localization method for wireless sensor networks," *Eurasip Journal on Applied Signal Processing, Special Issue on Sensor Networks*. (submitted November 2001).

[16] H. L. Van Trees, *Detection, Estimation, and Modulation Theory: Part I*. New York: Wiley, 1968.

[17] P. B. van Wamelen, Z. Li, and S. S. Iyengar, "A fast algorithm for the point pattern matching problem," November 2000. preprint.

[18] J. D. Gorman and A. O. Hero, "Lower bounds for parametric estimation with constraints," *IEEE Transactions on Information Theory*, vol. 26, pp. 1285–1301, November 1990.

[19] T. L. Marzetta, "A simple derivation of the constrained multiple parameter cramer-rao bound," *IEEE Transactions on Signal Processing*, vol. 41, pp. 2247–2249, June 1993.

[20] P. Stoica and B. Ng, "On the cramer-rao bound under parametric constraints," vol. 5, pp. 177–179, July 1998.

[21] P. Stoica and T. L. Marzetta, "Parameter estimation problems with singular information matrices," *IEEE Transactions on Signal Processing*, vol. 49, pp. 87–90, January 2001.